

# INTEGRATION OF THOMSON SCATTERING AND LASER-INDUCED FLUORESCENCE IN ITER DIVERTOR

## *Engineering and Performance Analysis*

E.E. MUKHIN, G.S. KURSKIEV, D.S. SAMSONOV, S.YU. TOLSTYAKOV, A.G. RAZDOBARIN, N.A. BABINOV, A.N. BAZHENOV, I.M. BUKREEV, A.M. DMITRIEV, D.I. ELETS, A.N. KOVAL, A.E. LITVINOV, S.V. MASYUKEVICH, V.A. SENITCHENKOV, V.A. SOLOVEI, I.B. TERESCHENKO, L.A. VARSHAVCHIK

Ioffe Institute

St.Petersburg, Russia

Email: e.mukhin@mail.ioffe.ru

A.V. GORBUNOV, A.S. KUKUSHKIN, M.G. LEVASHOVA, V.S. LISITSA, K.YU. VUKOLOV

NRC Kurchatov Institute

Moscow, Russia

E.B. BERIK

ESTLA Ltd

Tartu, Estonia

P.V. CHERNAKOV, AL.P. CHERNAKOV, AN.P. CHERNAKOV

Spectral-Tech, ZAO

St. Petersburg, Russia

A.N. MOKEEV

Institution 'Project Center ITER' RF DA

Moscow, Russia

P.ANDREW, M. KEMPENAARS, G. VAYAKIS, M.J. WALSH

ITER Organization

St. Paul Lez Durance Cedex, France

## **Abstract**

DTS and LIF are both laser aided diagnostics; hence, it seems attractive to combine the systems using universal laser and probing optics, which is the most sophisticated and expensive part of any ITER optical diagnostics. The paper discusses the benefits of divertor Thomson scattering 55.C4 (DTS) and laser-induced fluorescence 55.EA (LIF) integration in the divertor port #8 of ITER. The combined DTS/LIF diagnostic provides simultaneous measurements of the local  $T_e$ ,  $n_e$ ,  $T_i$ ,  $n_i$  and  $n_{He/H/D/T}$  along the probing laser paths. The set of plasma parameters allows calculating rates of the processes important for better understanding physics of divertor operational modes.

## 1. INTRODUCTION

The ITER divertor Thomson scattering (DTS) and Laser-induced Fluorescence (LIF) are active laser-aided diagnostics providing local measurements of plasma parameters in the outer divertor leg. The routinely used in tokamak plasmas, Thomson scattering (TS) measures electron density ( $n_e$ ) via the integrated TS spectrum and temperature ( $T_e$ ) - via the TS spectrum shape. Main challenges and capabilities of DTS in the ITER divertor were described previously [1]. Unlike Thomson scattering on free electrons, LIF measures line emission of atoms or ions having bound electrons. The fluorescence is induced by laser photons with an energy corresponding to the energy gap between bound electron states. The main tasks of the LIF in ITER divertor are to measure ion temperature ( $T_i$ ) using Doppler broadening of the HeII ion spectral lines and helium density ( $n_{He}$ ) from the atomic helium line intensity (see details in [2]). The atom (ion) density measurement is based on the collisional-radiative model (CRM) establishing relationship between the density and the excited level population measured by LIF. The CRM simulation requires input information about local electron parameters  $T_e$  and  $n_e$  provided by DTS. One of the most important parameters for edge tokamak plasmas is the main component (H/D/T) atomic density. The neutral hydrogen density in a tokamak was first measured in Ioffe Institute [3]. This pioneering paper devoted to

the first implementation of LIF in tokamak where radiation at  $H_\alpha$  (656.3 nm) was used for both pumping and measured induced fluorescence corresponding to the optical transition between 2<sup>nd</sup> and 3<sup>rd</sup> excited levels. The LIF diagnostic with pumped transition 2-3 is not a routine due to coinciding pumping and measured wavelengths and, thus, strong influence of stray-scattered laser radiation, which cannot be rejected by spectral filtering alone. An extension of LIF was the laser induced ionization (LII) using bound-free transition, where ionization of the hydrogen 4<sup>th</sup> atomic state provided by powerful DTS laser (1064 nm) gives quench of the  $H_\beta$  (486.1 nm) local radiation [4]. Below we first present measurements using another kind of LIF - laser induced quenching (LIQ) measurements of  $n_D$  based on quench of the  $D_\alpha$  radiation caused by pumping transition from 3<sup>rd</sup> to one of the upper atomic hydrogen levels with wavelengths shifted from  $D_\alpha$  by hundreds of nm. Summarizing, the combined DTS and different kinds of LIF approaches simultaneously measure a set of electron, ion and atom parameters ( $T_e$ ,  $n_e$ ,  $T_i$ ,  $n_i$  and  $n_{He/H/D/T}$ ) localized in 24 spatially resolved elements arranged along the laser beams nearly parallel to magnetic surfaces, thus locating an ionization front with precision on the order of  $\sim 25$  mm. These plasma parameters help to better understand physics of detachment through assessing electron process rates, including ionization, recombination and radiation rates, which play an important role in the cooling and recombination of the plasma flow, and ion-neutral collisions, being not directly involved in the reduction of the plasma flux to the target but playing three important roles in the detachment physics: (1) control effective pressure in the recycling region, with counter-balancing the upstream plasma pressure; (2) cool the plasma down to  $\sim 1$  eV and initiate the recombination processes; (3) ‘friction’ switch the plasma flow from free streaming to diffusion, making the residence time of the electrons and ions sufficient for recombination [5]. Under detachment, the input plasma flux from the upstream core plasma (free streaming) must undergo the following sequential changes: slowing down from free flow to slow diffusion; cooling down to  $\sim 1$  eV and finally recombining. All three phenomena are necessary to effectively reduce heat loading on the divertor plates. In case of insufficient slowing down, the incoming flows will reach the divertor plates not cooled enough and without cooling, the kinetic energy of the flow at the wall will be too high. Effective volumetric recombination is possible only at plasma temperatures below  $\sim 1$  eV, and without recombination, each ion reaching the divertor plate will transfer  $\sim 13.6$  eV of the recombination energy in the form of heat, which is unacceptably high for the high-recycling mode. Therefore, there is an unmet demand for diagnostics able to locally determine plasma characteristics for simulating the reaction rates most important for the divertor physics, as follows:

- Rates of ionization and recombination ( $T_e$ ,  $n_e$ );
- Emission intensity ( $T_e$   $n_e$   $n_i$   $n_{He/H/D/T}$ );
- Frictional force of the plasma flow due to collisions with neutrals ( $T_i$   $n_i$   $n_{He/H/D/T}$ );
- Pressure of the incoming plasma flow ( $T_e$   $n_e$   $T_i$   $n_i$ ).

This paper is organized as follows: Section 1 gives a general description of the integrated DTS/LIF diagnostic ability and compares parameters to be measured with those required to describe physics of the divertor detachment. Section 2 is devoted to DTS, particularly Section 2.1 discusses technical requirements and peculiarities of the DTS implementation in the ITER divertor; Section 2.2 describes simulation of the DTS measurement accuracy over the  $T_e$  and  $n_e$  range of interest. In Section 3, possible widening of LIF abilities in the ITER divertor are discussed. In Section 3.1, abilities to measure  $n_e$  in the range of  $10^{18}$  -  $10^{20}$  m<sup>-3</sup> are analyzed using the temporal behavior of HeI fluorescence based on specially developed HeI CRM. Section 3.2 reviews the ability to measure atomic hydrogen density in the edge tokamak plasma. The paper concludes with a summary of the current ITER DTS/LIF status and indicates options for further evolution of the system.

## 2. THOMSON SCATTERING IN ITER DIVERTOR

The DTS/LIF optical layout uses crossed probing and viewing beams with the front-end laser launcher located beneath the divertor cassettes and the first collecting mirrors near the side wall of divertor port. The laser beam enters along the bottom of the divertor cassette and, then, comes upwards into the outer divertor SOL, passing through the gap between adjacent divertor cassettes #21 and #22. Several interchangeable probing chords with the same collection optics should improve reliability of the diagnostics. All the mirrors are protected from deposits / sputtering by thin quartz windows; of them, laser windows will be self-cleaned by the probing lasers themselves [6] and the collection window will be cleaned by RF plasma discharge (out of the scope of this paper). Laser chords launched by First Laser Mirror (FLM) 1 (laser paths #1 in Fig. 1) are very close to the separatrix, coinciding with the main stream to the outer divertor leg, and are the most informative for the detachment monitoring and control. Laser beams launched by FLM 2 (laser paths #2) and FLM 3 (laser paths #3) are less informative but located further from the outer divertor target in the less polluted region. The probing beams launched from FLM 3 are eligible only for measurements near the strike point. Optical parameters of the collection system are shown in Fig. 2.

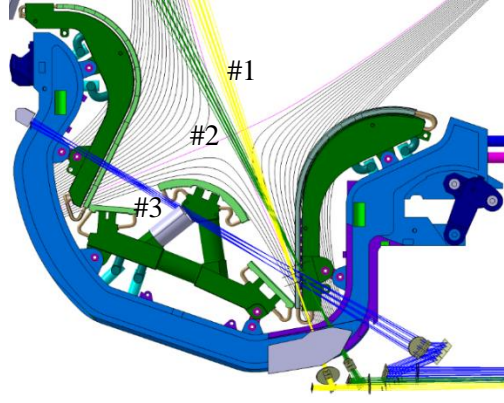


FIG. 1. Relative location of DTS/LIF probing chords and magnetic field surfaces in outer divertor leg.

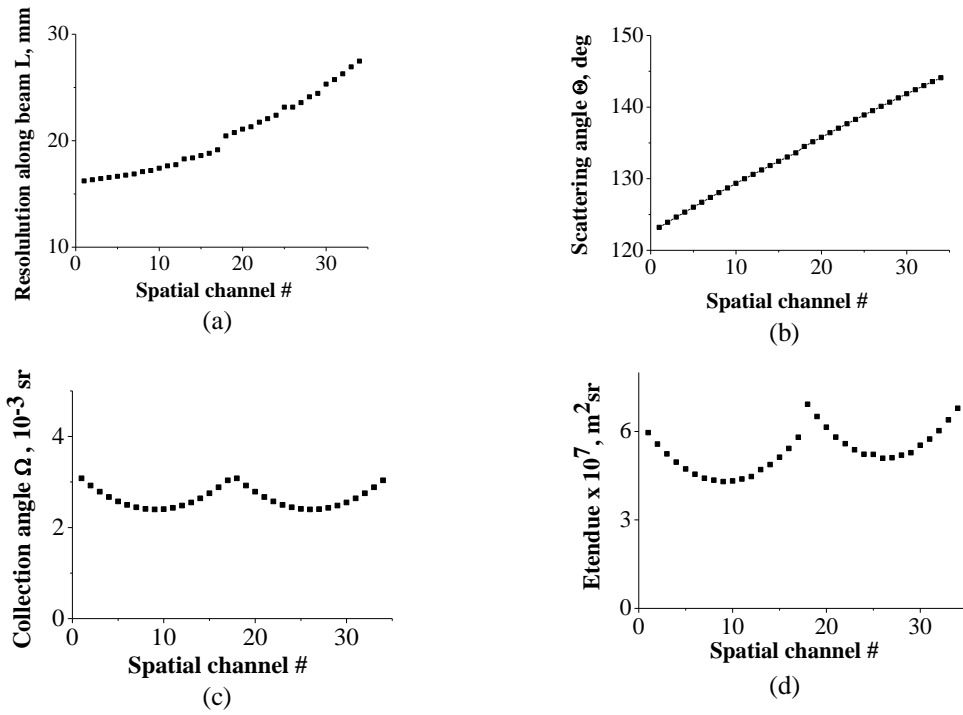


FIG. 2. Variation of the collection system optical parameters in different spatial channels. The spatial channel numbers are laid out along the probing chords #1 (see FIG. 1) from the outer divertor leg bottom: (a) – Scattering length, (b) – Angle of scattering, (c) – Collection solid angle, (d) – Etendue.

One of the main challenges for the DTS system is extremely high-electron-density and low-electron-temperature plasmas in the regions with predominant recombination. Such a cool and dense plasma leads to the Debye length approaching the change in the scattered wave vector and the deviation of the TS spectrum shape from Gaussian becomes very pronounced. Therefore, standard TS signal processing algorithm using separation of variables  $T_e$  and  $n_e$ , which is valid for light scattering on free electrons, is not valid because both the TS spectrum shape and the integral of TS spectrum are the functions of  $n_e$  and  $T_e$ . The influence of collective effects on TS cross section are taken into account by the following equations [7]:

$$\frac{d\sigma_\omega}{d\omega d\Phi} = \frac{e^4}{m^2 c^4} \frac{1}{\sqrt{\pi}} \left[ \frac{\Gamma_\alpha(x)}{\omega_e} + Z \left( \frac{\alpha^2}{1+\alpha^2} \right) \frac{\Gamma_\beta(y)}{\omega_i} \right]; \quad (1)$$

where

$$\Gamma_{\alpha}(x) = \frac{\exp(-x^2)}{\left[1 - \alpha^2 \left(2x \int_0^x \exp(t^2 - x^2) dt - 1\right)\right]^2 + \pi \alpha^4 x^2 \exp(-2x^2)},$$

$x = \Omega / \omega_e$ ;  $y = \Omega / \omega_i$ ;  $\Omega = \omega - \omega_0$ , where  $\omega$  and  $\omega_0$  – frequency for the scattered and incident radiation;

$$\omega_e = \frac{2\omega}{c} \sqrt{\frac{2kT_e}{m}} \sin\left(\frac{\theta}{2}\right); \quad \omega_i = \frac{2\omega}{c} \sqrt{\frac{2kT_i}{M}} \sin\left(\frac{\theta}{2}\right); \quad \alpha = \frac{c}{\omega \sin(\theta/2)} \sqrt{\frac{\pi n_e e^2}{kT_e}}; \quad \beta^2 = Z \frac{T_e}{T_i} \frac{\alpha^2}{1 + \alpha^2}$$

$c$  – speed of light in a vacuum,  $T_e$ ,  $T_i$  – electron and ion temperature,  $Z$  – ion charge,  $n_e$  – electron density,  $k$  – Boltzmann constant,  $m$  and  $M$  – electron and ion mass,  $e$  – electron charge,  $\theta$  – angle of scattering; other variables are arbitrary and expressed using the above described.

Performance analysis of the DTS diagnostic using both an analytical approach and a numerical technique were developed previously for the ITER core plasma [8] for managing the deviation of the electron velocity distribution function from a Maxwellian caused by relativistic effects and high-power heating. It is shown below that the suggested approach to  $T_e$  and  $n_e$  simulation provides accuracy quite better than the technical requirements, in spite of the pronounced collective effects. Cases with low  $n_e$  and classical TS spectra, where the diagnostics performance degrades significantly (though within the technical requirements) can benefit from DTS / LIF integration (see Section 3.2).

### 2.1. Technical requirements for DTS

Extremely high density ( $< 2 \cdot 10^{21} \text{m}^{-3}$ ) and low temperatures ( $> 0.3 \text{ eV}$ ) are expected in the vicinity of strike point close to the divertor targets, while for the upper part of the chord the variation of  $n_e$  and  $T_e$  is low and ranges of variation are quite usual for edge tokamak plasmas. The lower part of the probing chord covering 4 spatial points at the distance of  $\sim 0.75 \text{ m}$  from the launcher position is characterized with: high density  $n_e = 2 \cdot 10^{20} - 2 \cdot 10^{21} \text{ m}^{-3}$ ; extremely low to moderate temperature  $T_e = 0.3 - 40 \text{ eV}$ ; Salpeter parameter (defined as the inverse product of the change in the scattered wave vector times the plasma Debye length) is as high as unity; therefore, collective effects should be taken into account. At the very low temperatures, corresponding to the region, one of the most important roles of the DTS will be to provide experimental evidence that strong recombination is occurring in the target vicinity and to validate plasma boundary code simulations of the detachment behaviour. Since the recombination rate increases more rapidly in the region with  $T_e$  below  $\sim 0.5 \text{ eV}$ , it suffices for code validation to provide a measurement of  $T_e \sim 0.3 - 1 \text{ eV}$  with accuracy  $0.2 \text{ eV}$ . All other values of  $T_e$  and  $n_e$  have to be measured with accuracy no more than 20%. The upper part of the chord covering 20 spatial points is characterized with: moderate density range  $n_e = 0.5 \cdot 10^{19} - 2 \cdot 10^{20} \text{ m}^{-3}$  and moderate temperature  $T_e = 5 - 200 \text{ eV}$ ; thus, no collective effects are expected. Summarizing all the above, the conditions for the upper and lower parts of the chord are very different, and different approaches should be considered. Standard TS polychromators are used to analyse scattered spectra from the upper part of the chord, while for the lower part, where collective effects are expected, we are planning to use special polychromator with better spectral resolution.

### 2.2. DTS measurement capability

Taking into account the need for a  $T_e$  measurement below  $200 \text{ eV}$ , background radiation emitted in the diagnostic working range  $1 - 1.06 \mu\text{m}$  should be considered when designing the ITER DTS. The background radiation intensity varies very slowly compared with the laser pulse duration (3 ns), and this virtually constant background can be rejected using a simple low-frequency filter. Such approach saving dynamic range of detectors cannot remove shot noise, which is proportional to the square root of the signal intensity and reduces the accuracy of the  $T_e$  and  $n_e$  measurements. According to analysis of the background radiation in the DTS working spectral range presented in our previous papers [1, 9, 10], blackbody radiation resulting from intense plasma heating of the divertor targets and line radiation appearing in nitrogen seeded plasma can be limiting background components. Nitrogen, injected into the divertor region to provide the radiative dissipation necessary to achieve plasma detachment, has spectral line at  $\sim 1.011 \mu\text{m}$  with intensity  $\sim 10$  times higher than the expected TS signal integrated over a  $15 \text{ nm}$  spectral interval. The intense impurity line radiation will be rejected using special notch filters or arranging the spectral line between spectral channels. To minimize the blackbody background, the cone of the collection solid angle is centred on the gap between divertor cassettes. This observation geometry prevents direct viewing of heated surfaces or surfaces from which reflection of the radiation may occur, this helps to avoid polluting the TS signal with blackbody radiation. The expected  $n_e$  and  $T_e$  errors in the vicinity of outer strike point were assessed using the following algorithm: (a) estimation of the expected TS signals in spectral channels based on the known engineering parameters and using TS spectra shape calculated by equation (1); (b) multiple solution

( $10^3$  runs) of the inverse problem of the recovery of  $T_e$  and  $n_e$  from the TS signals simulated for given  $n_e$  and  $T_e$  with allowance for random deviations described by equation (2) in [8]; (c) standard deviation distribution functions of the measured  $T_e$  and  $n_e$ , as well as the expected measurement accuracy. The errors for the lower part of the chord are summarized in Fig. 3. According to SOLPS modelling, the minimum density for the lower part of the chord is expected to be rather high  $> 2 \cdot 10^{20} \text{ m}^{-3}$ . Such high  $n_e$  significantly increases scattered signal, thus improving measurement accuracy. However, to estimate  $T_e$  and  $n_e$  errors we suggest measurement accuracy of the TS signal to be not less than 2.5%, assuming probable systematic errors. Fig. 3a shows that for  $n_e > 2 \cdot 10^{20} \text{ m}^{-3}$ , the estimated errors of both  $n_e$  and  $T_e$  satisfy the requirements in the entire  $T_e$  range. Fig. 3b shows that the measurement accuracy of  $T_e=0.3 \text{ eV}$  meets the requirements of 0.2 eV accuracy throughout the entire  $n_e$  range with lower limit of  $n_e=1.2 \cdot 10^{19} \text{ m}^{-3}$ . The standard approach to analyse the DTS capabilities in the upper part of the probing chord shows that the diagnostics performance degrades (compare Fig. 3 and 4) though still meets the technical requirements.

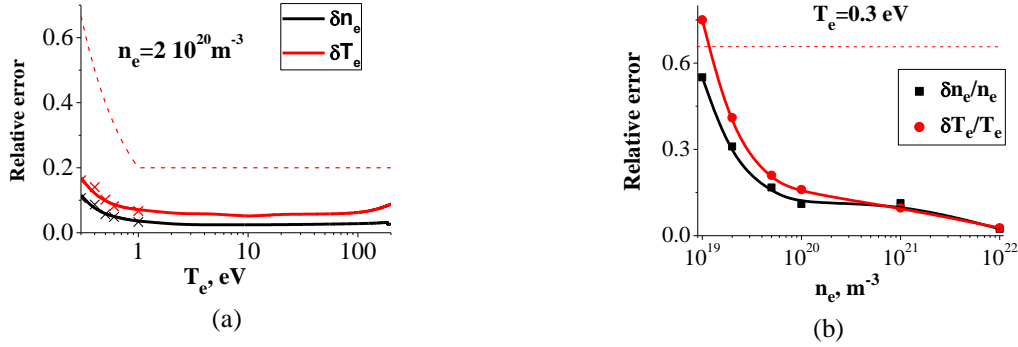


FIG. 3. Relative errors of  $n_e$  and  $T_e$  measurements in the vicinity of the strike point. Background radiation intensity was scaled from SOLPS run #1514 matching  $n_e^2$  dependence. The dashed line marks the acceptable accuracy. (a) Expected errors for  $T_e$  and  $n_e$  in case of minimum (according to SOLPS run #1514) density  $2 \cdot 10^{20} \text{ m}^{-3}$ . Solid curves – analytical approximation, crosses – errors estimated using numerical experiment; (b) Errors for  $T_e$  and  $n_e$  in the case of  $T_e=0.3 \text{ eV}$  for various densities.

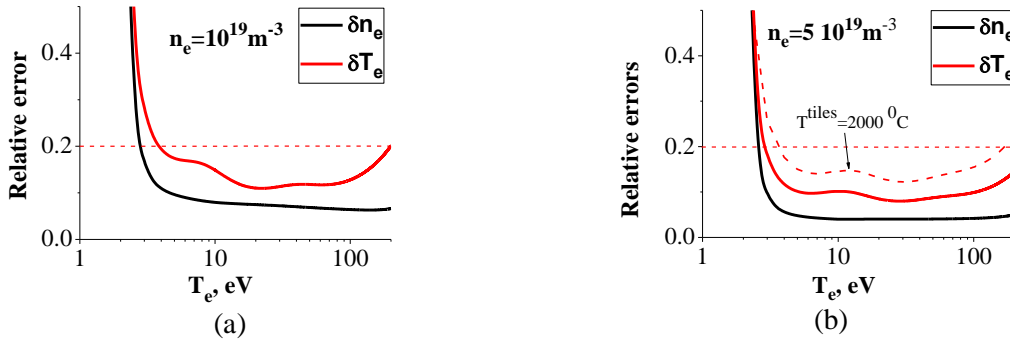


FIG. 4. Relative errors for the TS measurements on the upper part of the chord. (a) - for  $n_e=10^{19} \text{ m}^{-3}$ , which is minimum density from the technical requirements. The continuum background is taken from (b); (b) – for  $n_e=5 \cdot 10^{19} \text{ m}^{-3}$ , which is the minimum density predicted in the outer divertor by SOLPS run #1514 yielding peak power flux densities of  $8 \text{ MW/m}^2$ . The dashed line corresponds to the case when blackbody radiation for divertor tiles temperature  $2000 \text{ C}$  is taken into account. The continuum background is 5-fold overestimated against that calculated for the run.

### 3. LIF IMPLEMENTATION IN ITER DIVERTOR

Currently, the primary role of LIF is to supplement measurements of  $n_{\text{HeI}}$  distribution for assessing helium ash removal (group 1a – Basic Control). Secondly, LIF is the backup diagnostics for measuring  $T_i$  in the divertor (group 2 - Physics). A detailed description of the method ability to meet the requirements is presented in [2]. Below we are focusing on two approaches expanding the LIF capabilities: measuring  $n_e$  to improve capability of DTS and measuring the main component (H/D/T) atomic density.

#### 3.1 LIF for measurement of electron density

Short laser pulses comparable to, or shorter than the lifetime of the excited states are used to measure plasma parameters and analyse the fluorescence pulse shapes. Using He I structure of excited states (singlets and triplets),

simulation of  $n_e$  from the fluorescence signal shape can be performed. The dynamic collisional-radiative model (DCRM) developed for He I describes temporal behaviour of the fluorescence signals depending on the laser pulse shape, exciting transition and local values of  $n_e$  and  $T_e$ . The DCRM simulation was made for helium triplet line 587.6 nm (transition  $1s3d\ 3D \rightarrow 1s2p\ 3P$ ) under the following plasma parameters:  $n_e = 10^{17}$ - $10^{21}\ \text{m}^{-3}$  and  $T_e = 0.3$ - $300\ \text{eV}$ , assuming the excitation of the triplet line 388.9 nm ( $1s2s\ 3S \rightarrow 1s3p\ 3P$ ) via laser with pulse duration  $\tau_l = 10\ \text{ns}$ , energy  $E_l = 1\ \text{mJ}$ , spectral linewidth  $\Delta\lambda_l = 1000\ \text{pm}$  and beam cross section  $S = 1\ \text{cm}^2$ . The laser power spectral density was described by a peak function similar to those for optical parametric oscillator (OPO) or dye laser pulses. The influence of the laser pulse temporal shape and, especially, the pulse wings affecting the fluorescence response were taken into account. The simulation shows that the fluorescence duration (FWHM) varies from 10 to 100 ns over  $n_e$  range of  $10^{17}$ - $10^{21}\ \text{m}^{-3}$ , while the dependence on  $T_e$  in the range from 1 to 10 eV is much weaker (see Fig. 5) and can be neglected for the SOL plasma parameters. Thus,  $n_e$  in SOL plasma can be estimated from the fluorescence signals without measured  $T_e$ . The effect of  $T_e$  becomes significant near separatrix with  $T_e > 10\ \text{eV}$  or in divertor areas with  $n_e > 3 \cdot 10^{20}\ \text{m}^{-3}$ , where standard TS approach has adequate accuracy (see Fig. 4(b)) and doesn't require the auxiliary LIF data.

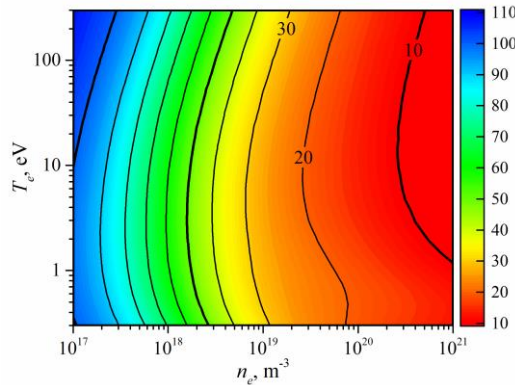


FIG. 5. Duration of fluorescence signal on the He I line 587.6 nm as a function of  $n_e$  and  $T_e$  for excitation on the line 388.9 nm with the following laser pulse characteristics:  $\tau_l = 10\ \text{ns}$ ,  $E_l = 1\ \text{mJ}$ ,  $\Delta\lambda_l = 50\ \text{pm}$  and  $S = 1\ \text{cm}^2$

The LIF measurement of  $n_e$  in the plasma core  $r/a=0.7$  of the Globus-M tokamak was performed using TS diagnostic collection optics. The laser beam was launched horizontally through the equatorial port using TS laser beam injection geometry (see Fig. 6). The LIF signal was collected with the high-aperture TS objective and transmitted to the diagnostic room by the TS optical fiber bundle and filtered by the 10 nm bandpass filter. The data acquisition system consists of photomultiplier and high-speed ADC (5GS/s, 500MHz bandwidth). The measurements were carried out in ohmic discharges ( $B_{\text{Tor}} = 0.47\ \text{T}$ ,  $I_p = 190\ \text{kA}$ ) with additional helium puffing. The reference measurements of  $n_e$  and  $T_e$  were performed with TS diagnostics. The narrow-band 100 Hz dye laser (ESTLA Ltd. DLC-N) used for excitation of HeI transition  $1s2s\ 3S \rightarrow 1s3p\ 3P$  (388.9 nm) has the following parameters: pulse energy in plasma  $E_l \approx 1\ \text{mJ}$ , duration  $\tau_l \approx 8\ \text{ns}$ , spectral linewidth  $\Delta\lambda_l \approx 50\ \text{pm}$ . Cylindrical lens telescope situated on the LIF laser output provides  $1.5 \times 1\ \text{cm}^2$  laser beam cross section in the observation point.

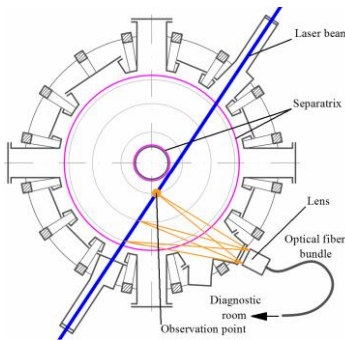


FIG. 6. Optical layout of LIF experiment on the Globus-M tokamak.

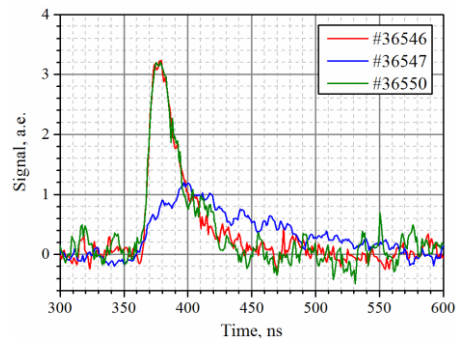


FIG. 7. LIF signals of He I line 587.6 nm. Note, all curves are normalized by integral area to unity.

Helium was injected at 60 ms in to the tokamak discharges #36546-36550. Three of the LIF signals are shown in Fig. 7. The fluorescence signal in discharge #36547 is longer than that in #36546 and #36550, i.e.  $n_e$  in #36547 is much lower than in #36546 and #36550. TS-derived  $T_e$  in the observation point was  $\sim 110\ \text{eV}$  for all discharges, resulting in  $n_e = (2.00 \pm 0.65) \times 10^{19}\ \text{m}^{-3}$  that corresponds to LIF signal duration measured in #36546 Globus discharge. This  $n_e$  correlates well with TS-derived one at the neighboring spatial point  $n_e = (2.4 \pm 0.2) \times 10^{19}\ \text{m}^{-3}$ .

Measured and CRM modelled fluorescence signals for  $n_e = 2 \cdot 10^{19} \text{ m}^{-3}$  and  $T_e = 110 \text{ eV}$  are shown in Fig. 8. Assuming  $T_e = 110 \text{ eV}$  in discharge #36547, an estimated  $n_e = (1.71 \pm 2.96) \times 10^{17} \text{ m}^{-3}$ . The higher relative error  $\Delta n_e$  corresponds to the low  $n_e$ , since in this case the relaxation of the excited level population and, hence, the fluorescence signal duration is mainly determined by spontaneous emission. The lower electron density in #36547 measured with LIF is consistent with the interferometer data.

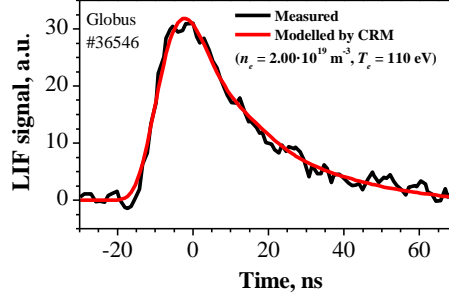


FIG. 8. LIF signals for  $n_e = 2 \cdot 10^{19} \text{ m}^{-3}$  and  $T_e = 110 \text{ eV}$ . Experimental curve measured in Globus-M discharge #36546 compared with the signal simulated by DCRM for HeI.

### 3.2 LIF for measurement of hydrogen isotope density

A novel LIF spectroscopic scheme based on laser induced quenching (LIQ) of the most intensive hydrogen line  $H_\alpha = 656.3 \text{ nm}$  is proposed. The idea is that the laser excites one of the allowed transitions from the  $n = 3$  state to one of the upper states (see Fig.9). During excitation, the population on the excited state with  $n = 3$  is reduced, thus the  $H_\alpha$  intensity decreases. Relative decrease of  $3^{\text{rd}}$  excited state population depends on the selected pumping transition and the laser power spectral density. The maximum quenching level may be estimated as  $I_{LIQ} = (g_3/g_{Up} + 1)^{-1}$ , where  $g_3 = 18$  and  $g_{Up}$  are the statistical weights of  $3^{\text{rd}}$  and upper states.  $D_\alpha$  line quenching was tested experimentally in a glow discharge plasma with laser exciting atomic deuterium from  $3^{\text{rd}}$  to one of the upper states with  $n = 4 \div 12$  (see Fig.10). In these experiments we used OPO laser pumped by  $3^{\text{rd}}$  harmonic of Nd:YAG.

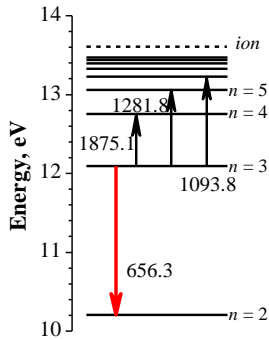


FIG. 9. Spectroscopic scheme for LIQ measurements of H/D/T

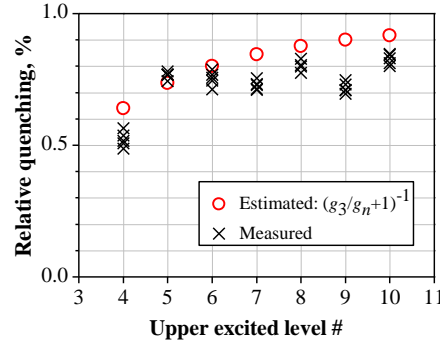


FIG. 10. Relative quenching level of  $D_\alpha$  by laser pumping to different upper states calculated (red o) and measured in glow discharge Deuterium lamp (black x)

Using atomic hydrogen CRM,  $H_\alpha$  intensity can be calculated for the DTS/LIF observation chords based on SOLPS simulated plasma parameters. The estimated background radiation collected on a detector is in the order of  $I_{BG} \sim 2.5 \cdot 10^{14} \text{ photons/s}$ . Accuracy of the hydrogen density measurements depends on the LIQ signal (SLIQ) and the background radiation intensity ( $I_{BG}$ ) at the  $H_\alpha$  line. SLIQ is proportional to the atoms density  $n_a(\text{HI})$  and depends on  $n_i$ ,  $n_e$ ,  $T_e$ , as well as spectroscopic scheme and the pumping laser pulse parameters. HI dynamic CRM was used to calculate the expected LIQ signals for the plasma parameters in the ITER divertor ( $n_e$  and  $T_e$ ,  $n_i(\text{HI}) = n_e$ ). The geometry factors (observation point height 2.5 cm and width 1 cm, laser beam cross section  $S = 1.5 \text{ cm}^2$ , solid angle  $\Omega = 5 \cdot 10^{-3} \text{ sr}$ ) and the collection system transmission of 0.2 were considered. Duration of the quenching signal is  $\Delta\tau = 15 \text{ ns}$  and the quantum efficiency at 656 nm for a detector based on APD is  $Q \sim 82\%$ . Parameters of OPO laser with 1 kHz repetition rate, wavelength  $\lambda = 1281.8 \text{ nm}$ , pulse duration  $\tau = 10 \text{ ns}$ , energy  $E = 2 \text{ mJ}$  and spectral width  $\Delta\lambda = 2000 \text{ pm}$  were used for simulations. The  $n_e$  and  $T_e$  required for CRM and provided by DTS were obtained with repetition rate of 50 Hz (DTS diagnostics requirements). Thus, 1 kHz OPO laser makes it possible to accumulate 20 LIQ signals, thus improving measurement accuracy. According to the results of accuracy simulations for  $n_{H/D/T} = 10^{17} \text{ m}^{-3}$  (Fig. 11), most  $n_{H/D/T}$  values are within the area with expected relative measurement errors lower than 10%. The expected measurement accuracy for SOLPS run #1514(DT) considering

$n_{H/D/T}$  distribution along the probing beam and  $H_\alpha$  intensity for the observation chords or spatial channels is shown in Fig. 12;  $\Delta n_{H/D/T}$  is expected to be lower than 20% for  $n_{H/D/T} > 10^{16} \text{ m}^{-3}$ .

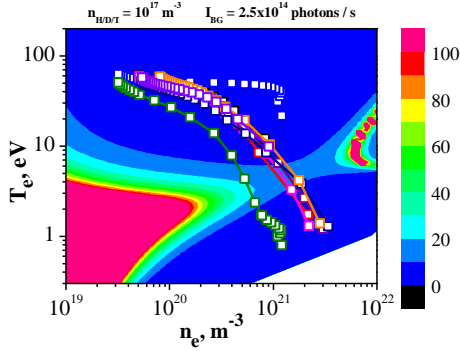


FIG. 11.  $n_{H/D/T}$  measurement accuracy (%) marked in specific colours, for  $n_{H/D/T} = 10^{17} \text{ m}^{-3}$  and  $I_{BG} \sim 2.5 \cdot 10^{14}$  photons/s in the observation points for several SOLPS runs #1511, #1514, #1537, #1538, #1540, #2501, #2505, #2530 and #2564.

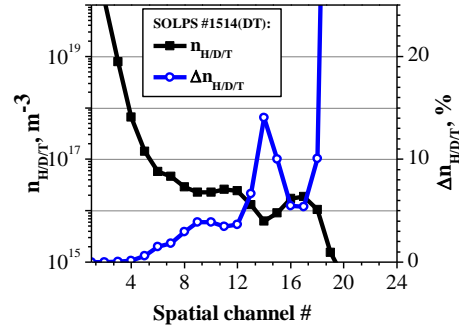


FIG. 12. Distribution of hydrogen density  $n_{H/D/T}$  and relative measurement accuracy  $\Delta n_{H/D/T}$  calculated for SOLPS run #1514. Pumping of  $n = 3 \rightarrow 5$  by a laser with  $\lambda = 1281.8 \text{ nm}$ ,  $\Delta\lambda = 2000 \text{ pm}$ ,  $\tau = 10 \text{ ns}$ ,  $E = 2.2 \text{ mJ}$ ,  $S = 1.5 \text{ cm}^2$ .

#### 4. CONCLUSION

The DTS/LIF diagnostic is able to simultaneously measure  $T_e$ ,  $n_e$ ,  $T_i$ ,  $n_i$  and  $n_{He/H/D/T}$  in ITER divertor SOL. The set of plasma parameters helps to simulate rates of ionization, recombination, radiation and ion-neutral collisions. Both DTS and LIF are laser-aided and use universal laser and probing optics. The main DTS challenge is to study extremely high-electron-density and low-electron-temperature plasmas in the regions with predominant recombination. TS spectra of cool and dense plasmas have complex shapes, which, as well as the TS spectrum integral depend on  $n_e$  and  $T_e$ ; hence, a conventional approach with separation of  $T_e$  and  $n_e$  variables doesn't work. Synthetic experiments show the expected  $T_e$  and  $n_e$  measurement accuracy to be much better than the specified technical requirements, in spite of the pronounced collective effects. In case of low  $n_e$ , when the classical TS spectrum is expected, the diagnostics performance degrades significantly, though still meets the technical requirements. The current LIF status implies: (a) measurements of  $n_{HeI}$  using a collisional-radiative model (CRM) to assess effectiveness of helium ash removal and (b) LIF as a backup diagnostics for divertor  $T_i$  measurements. We focus on the two approaches expanding LIF capabilities to measure the main component (H/D/T) atomic density and to measure  $n_e$  thus improving DTS capabilities. Temporal shapes of LIF-derived HeI fluorescence are able to expand the range and improve the accuracy of DTS-derived  $n_e$  based on HeI CRM and known  $T_e$ . The laser induced quenching (LIQ) of the most intensive hydrogen line  $H_\alpha = 656.1 \text{ nm}$  is proposed for measuring H/D/T atomic density.  $D_\alpha$  line quenching was tested experimentally in a glow discharge plasma with exciting transition from 3<sup>rd</sup> to one of the upper states with  $n = 4 \div 12$ . Further studies are needed for the combined DTS/LIF to become a routine diagnostics in tokamaks.

#### ACKNOWLEDGEMENTS

This report supported in part by Rosatom (contract - N.4a.241.19.18.1027) was prepared as an account of work for the ITER Organization. The views and opinions expressed herein do not necessarily reflect those of the ITER Organization.

- [1] MUKHIN, E., et al, Physical aspects of divertor Thomson scattering implementation on ITER, Nucl. Fusion **54** (2014) 043007.
- [2] GORBUNOV, A., et al, Laser-induced fluorescence for ITER divertor plasma, Fus. Eng. Design **123** (2017) 695.
- [3] RAZDOBARIN, G., et al, An absolute measurement of the neutral density profile in the tokamak plasma by resonance fluorescence on H-alpha line. Nucl. Fusion. **19** (1979) 1439.
- [4] GLADUSHCHAK, V., et al, Measurement of neutral density profile in a tokamak plasma using the principle of laser induced ionization, Nucl. Fusion **35** (1995) 1385.
- [5] KRASHENINNIKOV, S., KUKUSHKIN A., REVIEW Physics of ultimate detachment of a tokamak divertor plasma, J. Plasma Phys. **83** (2017) 1.
- [6] RAZDOBARIN, A., et al, Laser resistance of plasma-facing diagnostic components in ITER P4.215 SOFT (2018).
- [7] EVANS, D., KATZENSTEIN J., Laser light scattering in laboratory plasmas, Rep. Prog. Phys. **32** (1969) 207.
- [8] KURSKIEV, G., et al, A study of core Thomson scattering measurements in ITER using a multi-laser approach, Nucl. Fusion **55** (2015) 053024.
- [9] LISITSA, V. et al, Hydrogen lines in the infrared region and spectral background for the Thomson scattering diagnostics of the ITER divertor plasma, Plasma Phys. Rep. **38** (2012) 138.
- [10] LISITSA, V. et al, Spectroscopic problems in ITER diagnostics, Journal of Physics: Conference Series **397** (2012) 12015.